

Modeling of intersections using the nine-node assumed strain shell element

Przemysław Panasz¹ and Krzysztof Wiśniewski^{1*}

¹Department of Computational Science, Institute of Fundamental Technological Research, Polish Academy of Sciences
ul. Pawlowskiego 5B, 02-106 Warsaw, Poland
e-mail: ppanasz@ippt.gov.pl, kwisn@ippt.gov.pl

Abstract

The paper concerns modeling of intersections of shell structures using our 9-node quadrilateral shell element with 6 dofs/node, i.e including the drilling rotation, of [1]. The element is derived for the Reissner's kinematics from the potential energy functional extended by the Rotation Constraint applied by the penalty method. To avoid the membrane and transverse shear locking, the Assumed Strain method is used in the form described in detail in [1]. The formulation is based on the Green strain and is applicable to large strains and rotations. Two nonlinear numerical benchmarks are described: one with shell intersections (C-beam) and the other with drilling moment loading (L-shaped plate). They prove very good accuracy of our element, comparing to several reference elements.

Keywords: 9-node shell element, Assumed Strain method, drilling rotation, shell intersections

1. Introduction

In computational mechanics of plates and shells, it is important that rotational and translational degrees of freedom of intersecting elements were properly coupled. Theoretically, the shell elements with 6 dofs per node fulfill this requirement, but a lot depends also on a formulation and implementation of a finite element, in particular, of the part related to the drilling rotation. In this paper, we verify this feature of our element using some selected benchmarks.

2. Extended shell equations

We use a two-field extended functional including rotations,

$$F_2(\chi, \mathbf{Q}) \doteq \int_B \mathcal{W}(\mathbf{F}^T \mathbf{F}) dV + F_{RC} + F_{ext}, \quad (1)$$

where \mathcal{W} is the strain energy density. The Rotation Constraint (RC) $\text{skew}(\mathbf{Q}_0^T \mathbf{F}_0) = \mathbf{0}$ is applied as the penalty term,

$$F_{RC} \doteq \int_B \frac{\gamma}{2} \text{skew}(\mathbf{Q}_0^T \mathbf{F}_0) \cdot \text{skew}(\mathbf{Q}_0^T \mathbf{F}_0) dV, \quad (2)$$

where $\gamma \in (0, \infty)$ is the regularization parameter, see [2]. For shells, only the drilling rotation part of the RC is retained.

The position vector of an arbitrary point of a shell is defined by the Reissner hypothesis,

$$\mathbf{x}(\zeta) = \mathbf{x}_0 + \zeta \mathbf{Q}_0 \mathbf{t}_3, \quad (3)$$

where \mathbf{x}_0 is the position of the reference surface and \mathbf{Q}_0 is a rotation tensor constant over ζ . Besides, \mathbf{t}_3 is the shell director and h is the initial shell thickness. In the initial configuration, $\mathbf{Q}_0 = \mathbf{I}$.

Denote by ψ the canonical rotation pseudovector. Then, the rotation tensor $\mathbf{Q}_0 \in SO(3)$ is parameterized as follows

$$\mathbf{Q}_0(\psi) \doteq \mathbf{I} + \frac{\sin \omega}{\omega} \tilde{\psi} + \frac{1 - \cos \omega}{\omega^2} \tilde{\psi}^2, \quad (4)$$

where $\omega = \|\psi\| = \sqrt{\psi \cdot \psi} \geq 0$ and $\tilde{\psi} \doteq \psi \times \mathbf{I}$.

The Green strain tensor in the local Cartesian basis at the element's center $\{\mathbf{t}_k^c\}$ is obtained on use of

$$\mathbf{E} \doteq \frac{1}{2} (\mathbf{R}_{0c}^T \mathbf{F}^T \mathbf{F} \mathbf{R}_{0c} - \mathbf{I}), \quad (5)$$

where $\mathbf{R}_{0c} \in SO(3)$ is generated of the vectors \mathbf{t}_k^c , see [1]. For the Reissner's kinematics, the Green strain can be approximated linearly over the thickness, i.e. $\mathbf{E}(\zeta) \approx \boldsymbol{\varepsilon} + \zeta \boldsymbol{\kappa}$. Analytical integration over the thickness splits the shell strain energy density (per unit area of the reference surface) as follows: $\mathcal{W}_{sh} = \mathcal{W}_0 + \mathcal{W}_1$, where

$$\mathcal{W}_0 = h \left[\frac{1}{2} \lambda (\text{tr} \boldsymbol{\varepsilon})^2 + G \text{tr}(\boldsymbol{\varepsilon}^2) \right], \quad (6)$$

$$\mathcal{W}_1 = \frac{h^3}{12} \left[\frac{1}{2} \lambda (\text{tr} \boldsymbol{\kappa})^2 + G \text{tr}(\boldsymbol{\kappa}^2) \right]. \quad (7)$$

Note that \mathcal{W}_0 consists of the membrane and transverse shear energy while \mathcal{W}_1 of the bending and twisting energy.

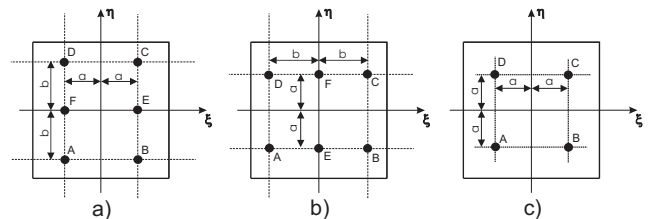


Figure 1: Sampling points of 9-node shell element: a) $\varepsilon_{11}, \varepsilon_{13}$ b) $\varepsilon_{22}, \varepsilon_{23}$ c) $\varepsilon_{12}, \kappa_{12}$

3. Formulation of our 9-node shell element

To avoid the membrane and transverse shear locking, we use the two-level strain approximations, which consist of sampling strain components at certain points and extrapolating these values over the element. This technique is called the Assumed Strain

*This research was partially supported by the Polish Ministry of Science and Higher Education under grant No. N501-290234.

(AS) method, and the variants of it described in the literature differ in the components which are sampled, the location of sampling points, and the extrapolation functions. In our 9-node shell element with drilling rotation of [1], designated as 9-AS, we use three sets of sampling points shown in Fig.1, where $a = \sqrt{1/3}$ and $b = \sqrt{3/5}$. The element is analytically integrated over the thickness while the 3×3 Gauss rule is used in the lamina.

4. Numerical benchmarks

In this section, we present numerical results for our 9-node element with drilling rotation designated as 9-AS. For comparison, we use the following 9-node elements: MITC9 of Adina, S9R5 of Abaqus and CAME9 of [3].

4.1. Channel section cantilever

A C-beam is fully clamped at one end and loaded by a vertical force P at the other, see Fig.2. A web and flanges of the beam intersect at 90 degrees so the shell elements with 5 dofs/node cannot be used. The data is as follows: $E = 10^7$, $\nu = 0.333$. Results of calculations are shown in Fig.3 and we see that the curves by our 9-AS element and the MITC9 element are close. For reference, the solution by the 16-node CAME16 element of [4] also is included. The solution by the S9R5 element is too soft.

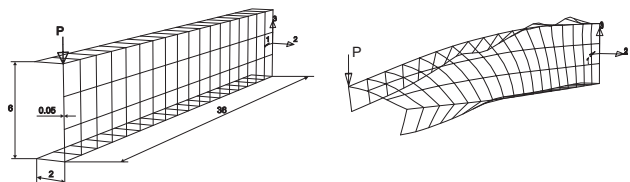


Figure 2: C-beam. Geometry and deformed configuration

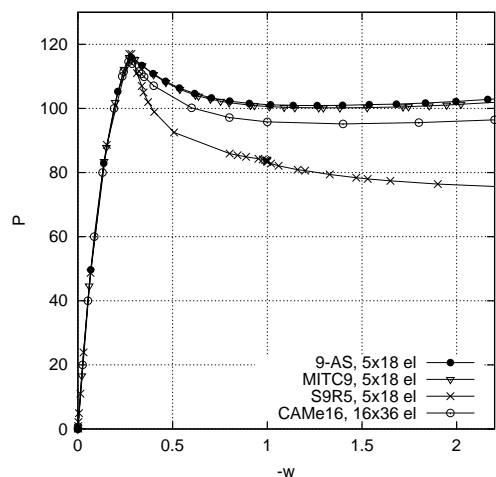


Figure 3: C-beam. Nonlinear solutions

4.2. L-shaped plate loaded by drilling moment

The L-shaped plate is clamped at one end and the drilling moment M is applied at the other, see Fig.4. The data is as follows: $E = 71240$, $\nu = 0.31$, $h = 0.6$. The drilling moment is applied using a layer of 'stiff' elements obtained by multiplying the Young's modulus by 10^5 .

The nonlinear solutions are shown in Fig.5 and we see that our 9-AS element gives very accurate results comparing to 3-node Timoshenko beam. The MITC9 and S9R5 elements fail

in this test. For reference, the solution by the 9-node CAME9 element of [3] is also included.

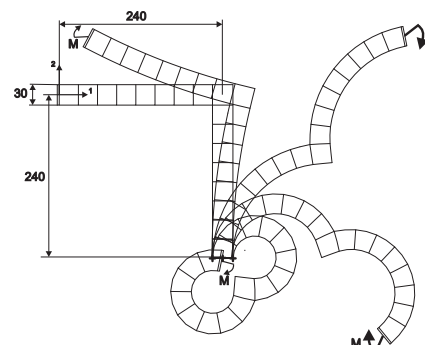


Figure 4: L-shaped plate. Initial and deformed shapes

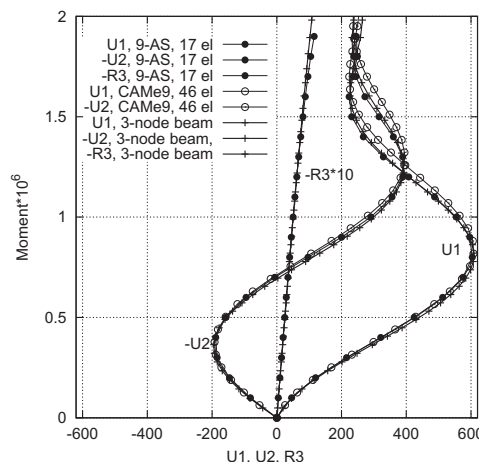


Figure 5: L-shaped plate. Nonlinear solutions up to 4π

5. Conclusions

The nonlinear benchmarks prove that the rotational and translational degrees of freedom of the 9-AS element are properly coupled. Hence, our 9-node Assumed Strain shell element with drilling rotation is a reliable tool which can be applied to a broader range of shell problems.

References

- [1] Panasz, P. and Wiśniewski, K.: *Nine-node shell elements with 6 dofs/node based on two-level approximations. Part I: Theory and linear tests*, Finite Element in Analysis and Design, Vol.44, pp. 784–796 (2008)
- [2] Wiśniewski K.: *Finite Rotation Shells. Basic Equations and Finite Elements for Reissner Kinematics*. CIMNE-Springer, 2010
- [3] Chróścielewski J., Makowski J., Pietraszkiewicz H.: *Statyka i Dynamika Powłok Wielopłatowych. Nieliniowa teoria i metoda elementów skończonych*. Biblioteka Mechaniki Stosowanej, IPPT PAN, Warszawa 2004
- [4] Chróścielewski, J. and Witkowski, W.: *Four-node semi-EAS element in six-field nonlinear theory of shells.*, Int. J. Num. Meth. Engng, Vol. 68, pp. 1137–1179, (2006)